

Activity of *Proteus mirabilis* FliL Is Viscosity Dependent and Requires Extragenic DNA

Yi-Ying Lee, Julius Patellis and Robert Belas
J. Bacteriol. 2013, 195(4):823. DOI: 10.1128/JB.02024-12.
Published Ahead of Print 7 December 2012.

Updated information and services can be found at:
<http://jb.asm.org/content/195/4/823>

SUPPLEMENTAL MATERIAL

These include:

[Supplemental material](#)

REFERENCES

This article cites 47 articles, 27 of which can be accessed free
at: <http://jb.asm.org/content/195/4/823#ref-list-1>

CONTENT ALERTS

Receive: RSS Feeds, eTOCs, free email alerts (when new
articles cite this article), [more»](#)

Information about commercial reprint orders: <http://journals.asm.org/site/misc/reprints.xhtml>
To subscribe to to another ASM Journal go to: <http://journals.asm.org/site/subscriptions/>

Activity of *Proteus mirabilis* FliL Is Viscosity Dependent and Requires Extragenic DNA

Yi-Ying Lee, Julius Patellis, Robert Belas

Department of Marine Biotechnology, University of Maryland Baltimore County, and Institute of Marine and Environmental Technology, Baltimore, Maryland, USA

Proteus mirabilis is a urinary tract pathogen and well known for its ability to move over agar surfaces by flagellum-dependent swarming motility. When *P. mirabilis* encounters a highly viscous environment, e.g., an agar surface, it differentiates from short rods with few flagella to elongated, highly flagellated cells that lack septa and contain multiple nucleoids. The bacteria detect a surface by monitoring the rotation of their flagellar motors. This process involves an enigmatic flagellar protein called FliL, the first gene in an operon (*fliLMNOPQR*) that encodes proteins of the flagellar rotor switch complex and flagellar export apparatus. We used a *fliL* knockout mutant to gain further insight into the function of FliL. Loss of FliL results in cells that cannot swarm (Swr^-) but do swim (Swm^+) and produces cells that look like wild-type swarmer cells, termed “pseudoswarmer cells,” that are elongated, contain multiple nucleoids, and lack septa. Unlike swarmer cells, pseudoswarmer cells are not hyperflagellated due to reduced expression of *flaA* (the gene encoding flagellin), despite an increased transcription of both *flhD* and *fliA*, two positive regulators of flagellar gene expression. We found that defects in *fliL* prevent viscosity-dependent sensing of a surface and viscosity-dependent induction of *flaA* transcription. Studies with *fliL* cells unexpectedly revealed that the *fliL* promoter, *fliL* coding region, and a portion of *fliM* DNA are needed to complement the Swr^- phenotype. The data support a dual role for FliL as a critical link in sensing a surface and in the maintenance of flagellar rod integrity.

Proteus mirabilis is a Gram-negative enteric gammaproteobacterium that is well known for its ability to move over nutrient agars by flagellum-dependent swarming motility and for its role as an opportunistic pathogen in urinary tract infections (UTIs) (1, 2). *P. mirabilis* is dimorphic and exhibits two cell morphotypes whose expression is dependent on the surrounding environment. In liquid environments, i.e., nutrient broths, *P. mirabilis* exists as a short vegetative swimmer cell that is 1.5 to 2.0 μm in length and possesses between 4 and 10 flagella per cell. When a swimmer cell encounters a viscous environment or a surface, e.g., nutrient agars, the swimmer cell differentiates into a swarmer cell 10 to 80 μm in length, with multiple evenly spaced nucleoids within its cytoplasm, that is propelled by hundreds or thousands of flagella per cell (1, 3, 4). Swarmer cells are uniquely adapted to life on surfaces (3, 5–8), and their ability to sense and respond to the host cell surface environment is thought to be critical in the regulation of several important virulence factors (1, 9–11).

Expression of the genes associated with swarmer cell differentiation is induced when a swimmer cell contacts a surface, and this effect is termed surface sensing (1, 4, 5). More than 50 genes, including flagellar and virulence genes, are involved in *P. mirabilis* swarmer cell differentiation (4, 12, 13). Expression of the swarmer cell regulon is controlled in large measure by FlhD_4C_2 , which is well-known as the master regulator of flagellar biosynthesis, acting to control a three-tiered hierarchical cascade of transcription (14–18). In this hierarchy, the *flhDC* operon (the sole member of class I) encodes the flagellar master regulator that in turn controls the expression of class II genes. Class II gene products include proteins for the assembly of the flagellar hook-basal body (HBB) complex, the type III protein export apparatus, and the regulators FliA and FlgM, which in turn control expression of class III genes (19, 20). Class III genes encode proteins required for later steps in flagellar assembly, including motor and chemotaxis proteins, flagellar filament-associated proteins, and flagellin (FlaA), the major protein of the flagellum (18, 20, 21). When *P. mirabilis* differenti-

ates from a swimmer to a swarmer cell, transcription at all levels of the flagellar regulon is upregulated to produce the hundreds of newly synthesized flagella on the swarmer cell (12, 13, 21). Inhibition of cell division and septation is also necessary to form polyploid swarmer cells and is controlled (in part) by FlhD_4C_2 (22).

Of the class II proteins, the function of FliL remains obscure. *fliL* is ubiquitous among the genomes of flagellated bacteria and is often the first gene in an operon (*fliLMNOPQR*) that encodes proteins of the cytoplasm-facing rotor switch complex known as the C-ring (FliM and FliN) and of the flagellar export apparatus (FliO, FliP, FliQ, and FliR) (23). FliL localizes to the inner membrane, in close proximity to the flagellar basal body (24–26). FliL is ca. 18 kDa, with a single transmembrane (TM) domain at its N terminus, suggesting that the N-terminal end of FliL resides in the cytoplasm while the rest of the protein is periplasmic.

Unlike other flagellar proteins, whose functions are conserved across motile bacterial species, *fliL* defects produce species-specific phenotypic changes. Several examples illustrate this. In the spirochete *Borrelia burgdorferi*, *fliL* mutants were observed to have defects in motility coupled with a reversal in the orientation of their periplasmic flagella (26). In alphaproteobacterial species, e.g., *Caulobacter crescentus*, *Silicibacter* sp. TM1040, and *Rhodobacter sphaeroides*, *fliL* null mutations result in a nonmotile phenotype (27–29), and *fliL* defects in *C. crescentus* result in the release of flagella (28). In enteric bacteria, e.g., *Escherichia coli* and

Received 23 October 2012 Accepted 4 December 2012

Published ahead of print 7 December 2012

Address correspondence to Robert Belas, belas@umbc.edu.

Supplemental material for this article may be found at <http://dx.doi.org/10.1128/JB.02024-12>.

Copyright © 2013, American Society for Microbiology. All Rights Reserved.

doi:10.1128/JB.02024-12

Salmonella enterica serovar Typhimurium (*Salmonella* herein), the loss of FliL does not affect swimming, but *fliL* cells have dramatic defects in swarming (24, 30). Similar to results in *C. crescentus*, *fliL* defects in *Salmonella* also result in detachment of flagella (24, 28), with breakage occurring between the proximal and distal rod proteins (FlgF and FlgG, respectively). Breakage of flagella in *fliL* cells has been hypothesized to be due to an increase in the torsional force on the basal body that results from the high viscosity associated with the surface of nutrient agar, which suggests that FliL functions in maintaining the integrity and stability of the flagellar rod (24, 31).

Belas and Suvanasuthi (32) reported that conditions that caused a stalling of *P. mirabilis* flagellar motors, e.g., by increasing the external viscosity or by addition of anti-FlaA antiserum to broths, induced swarmer cell differentiation and virulence gene expression (32). This result led to the hypothesis that the surface signal and inhibition of flagellar rotation are linked; however, the mechanism for signal propagation from the stalled flagellar motor to the cytoplasm is currently unknown.

More recently, we found that defects in *fliL* affect swarmer cell differentiation and result in the inappropriate production of elongated cells reminiscent of swarmer cells under noninducing conditions (nutrient broth growth). We refer to these elongated *fliL* cells as pseudoswarmers (12, 32), and their presence suggests that defects in *fliL* cause errors in sensing the surface signal that are manifested in transcriptomic changes (12).

Here, we used a *fliL* knockout mutant to gain further insight into the function of FliL. We show that loss of FliL results in cells that cannot swarm on agar surfaces (*Swr*⁻ phenotype) but swim in broth cultures (*Swm*⁺) and that pseudoswarmer cells present in liquid are elongated (*Elo*⁺), contain multiple, evenly spaced nucleoids, and lack septa, characteristics shared with swarmer cells. Unlike swarmer cells, pseudoswarmer cells are not hyperflagellated due to reduced expression of *flaA* (the gene encoding flagellin), despite an increased transcription of both *flhD* and *fliA*, two positive regulators of flagellar gene expression. Defects in *fliL* prevent viscosity-dependent sensing of a surface and viscosity-dependent induction of *flaA* transcription. Results from experiments designed to complement *fliL* and its *Swr*⁻ phenotype reveal a requirement of the *fliL* promoter, *fliL* coding region, and a portion of *fliM* DNA. The data support a dual role for FliL as a critical link in surface sensing and in the maintenance of flagellar rod integrity.

MATERIALS AND METHODS

Bacterial strains, plasmids, and growth conditions. Bacterial strains and plasmids used in this study are listed in Table 1. *P. mirabilis* BB2000 served as the wild type and the parent of all *P. mirabilis* mutants used in this study. *E. coli* XL1-Blue (Stratagene) was used for plasmid manipulations. Plasmids pACYC184 (37), pTrc99a (35), pBAD30, and pBAD33 (36) were used to express *fliL* in *trans*. *E. coli* and *P. mirabilis* were maintained in Luria-Bertani (LB) broth (10 g liter⁻¹ Bacto tryptone, 5 g liter⁻¹ yeast extract, 10 g liter⁻¹ sodium chloride) (39) or LB agar (LB medium containing 15 g liter⁻¹ Bacto agar) at 37°C. When isolated colonies of *P. mirabilis* were required, LSW⁻ agar (10 g liter⁻¹ Bacto tryptone, 5 g liter⁻¹ yeast extract, 0.4 g liter⁻¹ NaCl, 5 ml liter⁻¹ glycerol, 20 g liter⁻¹ Bacto agar) (33) was used to prevent swarming. Swimming motility was screened using Mot agar (10 g liter⁻¹ Bacto tryptone, 5 g liter⁻¹ NaCl, 3 g liter⁻¹ Bacto agar). As required, media were supplemented with 100 µg ml⁻¹ ampicillin, 40 µg ml⁻¹ chloramphenicol, and 50 µg ml⁻¹ kanamycin, respectively.

Construction of null mutations in BB2000. *fliL* null mutations in BB2000 were constructed by group II intron insertion (40) using a Targetron gene knockout system (Sigma-Aldrich) following the manufacturer's instructions. Plasmid pACD4K-C was used to construct the reprogrammed intron containing a kanamycin-resistant cassette. The intron was reprogrammed to insert between nucleotides (nt) 30 and 31 in *fliL*, producing plasmid pYL25. pYL25 and the intron expressing helper plasmid pAR1219 (34) were sequentially transformed into BB2000. Intron expression was induced by addition of isopropyl β-D-1-thiogalactopyranoside (IPTG), and isolates with the correct insertion of the intron were selected by kanamycin resistance. Plasmids pYL25 and pAR1219 were cured by passage of cells to nonselective medium several times followed by electroporation (41) and then by screening for loss of ampicillin and chloramphenicol resistance. The resulting null mutant was called YL1003 (*fliL::kan-nt30*) (where nt30 indicates the location of the intron insertion).

PMI3101, encoding the sole GGDEF-containing protein in the genome of *P. mirabilis*, was similarly knocked out at nt 166/167 using the same method.

The efficacy of the group II intron insertions was determined by PCR amplification and nucleotide sequencing. Primers used to reprogram the group II intron are listed in Table 2.

Complementation of *fliL* defects. Plasmids expressing *fliL* under the control of its native promoter (*P*_{*fliL*}) or inducible promoters (*P*_{*trc*} and *P*_{*BAD*}) were constructed as follows. *P*_{*fliL*}::*fliL*, including 200 bp upstream of the *fliL* start codon and going to the stop codon of *fliL*, was generated by PCR and ligated into the BamHI and HindIII sites in pACYC184. The resulting plasmid was called pYL30. For construction of *P*_{*trc*}::*fliL* and *P*_{*BAD*}::*fliL* expression plasmids, the same *fliL* codon region was generated by PCR and cloned into the NcoI and HindIII sites downstream of the *trc* promoter in pTrc99a or into the SacI and KpnI sites downstream of the *araBAD* promoter in pBAD36 or pBAD37, respectively. A plasmid containing the complete *fliL* operon was constructed by PCR amplification of a DNA fragment from 499 bp upstream of the start codon of *fliL* through the stop codon of *fliR*, followed by ligation into the BglI and Sall sites in pACYC184, resulting in plasmid pYL47.

Truncations of the *fliL* operon were made from pYL47 to remove *fliM*-*fliR* genes one after another, starting from the 3' end. Removal of *fliQ* and *fliR* genes in pYL47 was done by HindIII digestion, and the new plasmid was called pYL60 (see Fig. 6C). Removal of *fliP*-*fliR*, *fliO*-*fliR*, *fliN*-*fliR*, and *fliM*-*fliR* in pYL47 was achieved by reverse PCR with Phusion High-Fidelity DNA Polymerase (NEB), using one primer (pACYC184-HindIII_r) downstream of the *fliR* gene and the other (*fliO*-HindIII_r, *fliN*-HindIII_r, *fliM*-HindIII_r, and *fliL*-HindIII_r) on the 3' end of the *fliO*, *fliN*, *fliM*, and *fliL* genes, respectively. The PCR-generated DNA fragments were ligated following HindIII digestion to create pYL61, pYL62, pYL63, and pYL64 with deletions of *fliP*-*fliR*, *fliO*-*fliR*, *fliN*-*fliR*, and *fliM*-*fliR*, respectively (see Fig. 6C). Primers used for cloning are listed in Table 2. Each deletion in the *fliL* operon was confirmed by sequencing, after which the respective plasmids were separately transformed into YL1003, and the resulting swimming and swarming phenotypes were measured.

Ectopic single-copy expression of *P*_{*fliL*}::*fliL*. A method was developed to use Campbell-style single-crossover integration of a suicide plasmid containing *P*_{*fliL*}::*fliL* into an ectopic site on the *P. mirabilis* genome. A 2,183-bp fragment containing 1.5 kb of the PMI3101 gene (see Results), plus upstream sequence (PMI3099'-PMI3100-PMI3101) followed by *P*_{*fliL*}::*fliL*, was ligated into the SacI and EcoRI sites in the suicide vector pGP704 (38), resulting in pYL42. pYL42 was transferred to YL1003 via biparental mating between *E. coli* S17-1 λpir/pYL42 and YL1003, as previously described (33). The exconjugants were selected on LSW⁻ agar containing kanamycin and ampicillin. Complementation of the *Swr*⁻ defect in YL1003 was determined by measuring swarming motility on LB agar without antibiotic selection.

TABLE 1 Bacterial strains and plasmids used in this study

Strain or plasmid	Relevant characteristics ^a	Source or reference
Strains		
<i>P. mirabilis</i>		
BB2000	Wild type; spontaneous Rf ^r from PRM1	33
YL1003	<i>fliL::kan-nt30</i> ; BB2000 with group II intron insertion in the nt 30 of <i>fliL</i> , Km ^r	This study
YL1005	PMI3101:: <i>kan-nt166</i> , BB2000 with group II intron insertion in the nt 166 of PMI3101; Km ^r	This study
<i>E. coli</i>		
XL1-Blue	<i>recA1 endA1 gyrA96 thi-1 hsdR17 supE44 relA1 lac</i> [F' <i>proAB lacI^qZΔM15 Tn10</i> (Tc ^r)]	Stratagene
Plasmids		
pACD4K-C	Intron expression vector; p15A ori, Cm ^r	Sigma-Aldrich
pYL25	pACD4K-C containing retargeting intron specific to nt 30 of <i>P. mirabilis fliL</i> gene; Cm ^r	This study
pYL31	pACD4K-C containing retargeting intron specific to nt 166 of PMI3101; Cm ^r	This study
pARI1219	T7 RNA polymerase expression vector; pBR322 ori, Ap ^r	34
pTrc99a	<i>P_{trc}</i> expression vector; pBR322 ori, Ap ^r	35
pBAD30	<i>P_{BAD}</i> expression vector; p15A ori, Ap ^r	36
pBAD33	<i>P_{BAD}</i> expression vector; p15A ori, Cm ^r	36
pACYC184	Cloning vector; p15A ori, Cm ^r , Tc ^r	37
pYL30	pACYC184 containing a 699-bp DNA fragment containing <i>P_{fliL}</i> (200-bp upstream to the start codon), the codon region and 16 bp downstream <i>fliL</i> ; Cm ^r	This study
pYL35	pTrc99a containing <i>fliL</i> coding region, Ap ^r	This study
pYL36	pBAD30 containing the Shine-Dalgarno sequence and the codon region of <i>fliL</i> from pYL30, Ap ^r	This study
pYL37	pBAD33 containing the Shine-Dalgarno sequence and the codon region of <i>fliL</i> from pYL30, Cm ^r	This study
pYL47	pACYC184 containing <i>P_{fliL}</i> (487 bp upstream to the start codon of <i>fliL</i>) and codon region of the complete <i>fliLMNOPQR</i> operon, Cm ^r	This study
pYL60	pYL47 with deletion of HindIII fragment containing the <i>fliQR</i> codon region and 14 bp in the 3' end of the <i>flip</i> codon region, Cm ^r	This study
pYL61	pYL47 with deletion of the <i>fliPQR</i> codon region generated by PCR using pACYC184-HindIII_r and fliO-HindIII_f primers, Cm ^r	This study
pYL62	pYL47 with deletion of the <i>fliOPQR</i> codon region generated by PCR using pACYC184-HindIII_r and fliN-HindIII_r primers; Cm ^r	This study
pYL63	pYL47 with deletion of the <i>fliNOPQR</i> codon region generated by PCR using pACYC184-HindIII_r and fliM-HindIII_r primers, Cm ^r	This study
pYL64	pYL47 with deletion of the <i>fliPQR</i> codon region generated by PCR using pACYC184-HindIII_r and fliL-HindIII_r primers, Cm ^r	This study
pYL65	pTrc99a containing the codon region of <i>fliLM</i> , Ap ^r	This study
pYL66	pBAD30 containing the Shine-Dalgarno sequence and the codon region of <i>fliLM</i> ; Ap ^r	This study
pYL67	pBAD33 containing the Shine-Dalgarno sequence and the codon region of <i>fliLM</i> , Cm ^r	This study
pGP704	Suicide vector; R6K ori, Ap ^r	38
pYL42	pGP704 containing 1.5kb of PMI3099'-3101 immediately followed by <i>fliLp::fliL</i> from pYL30	This study
pYL70	pACYC184 containing <i>P_{fliA}::lacZ</i> fusion, Cm ^r	This study

^a Ap^r, Cm^r, Km^r, Rf^r, and Tc^r indicate ampicillin, chloramphenicol, kanamycin, rifampin, and tetracycline resistance, respectively.

Swimming and swarming motility assay. *P. mirabilis* cells were grown overnight in 2 ml of LB broth from a single colony. For bacterial cells prepared from broth, the overnight culture was inoculated into fresh LB broth at a 1:100 dilution and incubated at 37°C with shaking (200 rpm) for 2.75 h, when *fliL* strains produce the most pseudoswarmer cells in a population (12). For bacterial cells prepared from surfaces, 100 μl of an overnight culture was spread on the surface of LB agar in a 100-mm by 15-mm petri dish and incubated at 37°C for 4.5 h, when the wild-type strain BB2000 is actively swarming and produces the most swarmer cells in a population (data not shown). Cells were washed from the LB agar surface with 2 ml of 1 × phosphate-buffered saline (PBS) (8 g liter⁻¹ NaCl, 0.2 g liter⁻¹ KCl, 1.44 g liter⁻¹ Na₂HPO₄, 0.24 g liter⁻¹ KH₂PO₄).

Swimming motility was measured as the outward migration of the cells following point inoculation of an overnight culture in the center of a petri dish containing semisolid Mot agar and LB agar (0.3% agar). Swarming motility was measured as bacterial migration over the surface of LB agar. Swarming plates were made by dispensing 20 ml of sterilized molten LB agar medium in each 100-mm by 15-mm petri dish placed on a bench in a single layer. The agar was allowed to gel at room temperature for ca. 20 h before use. Swarming was assessed following inoculation of a 5-μl sam-

ple of bacteria from overnight cultures grown in LB broth. Swimming and swarming assays were conducted in an environmental chamber at 37°C with a constant humidity of 46%.

RNA extraction, cDNA synthesis, and quantitative RT-PCR. Total RNA was extracted and purified from bacterial samples using Ribopure (Ambion), following the manufacturer's instructions, with a 1-h DNase treatment. RNA was converted to cDNA using a high-capacity cDNA reverse transcription kit and RNase inhibitor (Applied Biosystems), with a thermocycling regime of 25°C for 10 min, 37°C for 2 h, and 85°C for 5 min. Quantitative reverse transcription-PCR (qRT-PCR) was performed using an ABI 7500 Fast real-time PCR system with the following thermocycling conditions: 95°C for 20 s, followed by 40 cycles of 95°C for 3 s and 60°C for 30 s. The change in target mRNA abundance was calculated using the 2^{-ΔΔC_T} formula (where C_T is threshold cycle) (42), with *rpoA* (RNA polymerase subunit alpha) serving as a control.

***P_{fliA}::lacZ* transcriptional fusion.** PCR was used to amplify the *fliA* promoter (386 bp 5' of the start of *fliA*). The resulting DNA was digested with BamHI and EcoRI and ligated into the BamHI and EcoRI sites 5' to a promoterless *lacZ* on pRS528 (43). The DNA fragment containing *P_{fliA}::lacZ* transcriptional fusion was generated by PCR and subcloned into the

TABLE 2 Oligonucleotide primers used in this study

Primer	Sequence (5'→3') ^a	Construct(s) or use
fliL30aEBS1d	CAGATTGTACAAATGTGGTGATAACAGATAAGTCGCTATAGCTAACTTACCTTTCTTTGT	YL1003
fliL30aEBS2	TGAACGCAAGTTTCTAATTTTCGATTTAATTTTCGATAGAGGAAAGTGTCT	YL1003
fliL30aIBS	AAAAAAGCTTATAAATTATCCTTAAATTACGCTATAGTCGCGCCAGATAGGGTG	YL1003
3101-166aEBS1d	CAGATTGTACAAATGTGGTGATAACAGATAAGTCATCTTTTATAACTTACCTTTCTTTGT	YL1005
3101-166aEBS2	TGAACGCAAGTTTCTAATTTTCGATTTAATTTTCGATAGAGGAAAGTGTCT	YL1005
3101-166aIBS	AAAAAAGCTTATAAATTATCCTTAAAGTTACATCTTTGTGCGCCAGATAGGGTG	YL1005
fliLpF	GGATCCGTGGTGTGCATATTT	Sequencing
fliLR	AGCGTAACGTGATCCCTATG	Sequencing
fliLp-BamHI_f	CTTGGATCCGTGGTGTGCATATTTTTG	pYL30
fliL-HindIII_r	CGGAAGCTTATCGCTCATAATGATTATC	pYL30, pYL35, pYL64
fliLup-BglI_f2	AATGCTCCTCGGCTCAATTACATCTTGCCTCTC	pYL47
fliR-SalI_r	CACGTCGACTCAAGAACTAATTGCTGCAA	pYL47
pACYC184-HindIII_r	CTACCGCATTAAAGCTTATCGATG	pYL61, pYL62, pYL63, pYL64
fliO-HindIII_r	ACTAAGCTTTTATGAGTTGCCTTTATCTCGC	pYL61
fliN-HindIII_r	ATTAAAGCTTTCACGACTCAGACGGCG	pYL62
fliM-HindIII_r	ATTAAGCTTCACTCATTGGTTTGTTCCTC	pYL63
fliL-NcoI_f	ATCCCATGGCTAATTACAGCAATGAACGTAA	pYL35
SacI-SD-fliL_f	CAAGAGCTCCACTACAAAACAGGAATTT	pYL36, pYL37
fliL-KpnI_r	CTTGGTACCTTATCGCTCATAATGATTATC	pYL36, pYL37
3101CO-SacI_f	CGGGAGCTCGGGTGATTATGCTGAAGATAATATG	pYL42
3101CO-SmaI_r	CCGCCCGGAAATATAGTGTATTTAATACTCTG	pYL42
fliLp-SmaI_f	TTTCCCGGGGTGGTGTGCATATTTTTGCC	pYL42
fliL-EcoRI_r	CCGGAATTCTTATCGCTCATAATGATTATC	pYL42
flaApF	GGATCCACTGGTCTCCTTTCT	pYL70
flaApEcoRI_r	AACGAATTCAGCTAGATTCCTTTAAAA	pYL70
lacZ-HindIII_r	TGATAAGCTTTTATTTTACACCCAGACCAACTGG	pYL70
fliL_r	GAGCATCTATCTCTGCCTGTGAAAGG-3'	qRT-PCR
flhDF	AAGGCTTCCGCAATGTTTAGAC	qRT-PCR
flhDR	GTTGCAAATCATCCACTCTGGA	qRT-PCR
fliAF	CCTGCGAGTGTGAATTGGA	qRT-PCR
fliAR	GGATTGTGTCACCTTCTCTTGC	qRT-PCR
fliMF	GTCATTCCGTATGGGGCTG	qRT-PCR
fliMR	AACCAGATTCGGCTCAAAGG	qRT-PCR
fliOF	CAACCTTTACCGTTGGACA	qRT-PCR
fliOR	CGACAACAGCTCTTTGGTA	qRT-PCR
flaAF	CAACTGAAGGTGCATTGAAC	qRT-PCR
flaAR	TGATTTCTCACCGCTCAGTA	qRT-PCR

^a Underlining indicates restriction sites for cloning.

BamHI and HindIII sites of pACYC184, resulting in pYL70. pYL70 was transformed into BB2000 or YL1003 by electroporation. Transcription of *flaA*, as measured by β -galactosidase activity, was determined using the Miller assay (44) as described previously (45), with cells harvested from the surface of LB agar after 4 h of incubation.

Protein sample preparation. Protein was obtained from 5 ml of 2.75-h broth cultures or 2-ml cell suspensions prepared from agar surfaces (described above). In both cases the suspended bacteria were centrifuged at 6,000 rpm for 10 min to obtain supernatant and cell pellet fractions. The pellets were washed with 1× PBS and then resuspended in 1 ml of 1× PBS. As required, wide-bore pipette tips were used to prevent shearing of cell-attached flagella. Whole-cell homogenates of the pellets were prepared by six cycles of sonication for 10 s followed by a pause on ice for 30 s. The protein concentration of all fractions was measured using a bicinchoninic acid (BCA) protein assay (Pierce).

Western blotting. The method described by Belas et al. (4) was used with Hybond-P polyvinylidene difluoride (PVDF) membranes (Amersham) and an ECL Plus system (GE Health Sciences). Flagellin (FlaA) was detected using rabbit polyvalent anti-FlaA antiserum (antiserum 497) (4) at a dilution of 1:5,000. FliM was detected with rabbit FliM antiserum (a gift from David Blair, University of Utah), using a 1:1,000 dilution of the stock. Horseradish peroxidase (HRP)-conjugated goat anti-rabbit IgG (Cell Signaling Technology) was used as the secondary antiserum at a titer

of 1:50,000 for FlaA and 1:10,000 for FliM antibodies. ImageJ (National Institutes of Health) software was used to determine protein abundance on the developed Western blots.

Fluorescent staining and microscopy. Bacterial cells were harvested from 2.75-h broth or 4.5-h plate cultures and resuspended in 500 μ l of 1× PBS using wide-bore tips to prevent shearing of the flagella. Bacterial cells were fixed by the addition of 3% (vol/vol; final concentration) paraformaldehyde (Sigma-Aldrich) to the cell suspension and incubation at room temperature for 10 min with gentle rocking. Fixed bacteria were stored at 4°C until use, at which time 50 μ l was placed on a poly-L-lysine-coated coverslip and left undisturbed at room temperature for 30 min. Nonadherent and loosely bound cells were removed by washing 10 times with 1× PBS. Cells bound to the coverslip were sequentially treated in 1-h steps with 50 μ l of 2% bovine serum albumin (BSA) in 1× PBS, followed by rabbit anti-FlaA antiserum (4) (1:100 in 2% BSA) and Alexa Fluor 568-conjugated goat anti-rabbit IgG (Invitrogen) (1:100 in 2% BSA). The coverslips were kept in a humidified chamber in the dark during the entire process. Each reagent was removed by copious washing with 1× PBS. FMI-43 (15 μ g ml⁻¹; Invitrogen) was used to label membranes, while bacterial nucleoids were stained using 4',6'-diamidino-2-phenylindole (DAPI) (2 μ g ml⁻¹; Invitrogen). Stained specimens were mounted in ProLong antifade reagent (Invitrogen), imaged using wide-field fluorescence microscopy with a Zeiss Axio Observer Z1 microscope and a

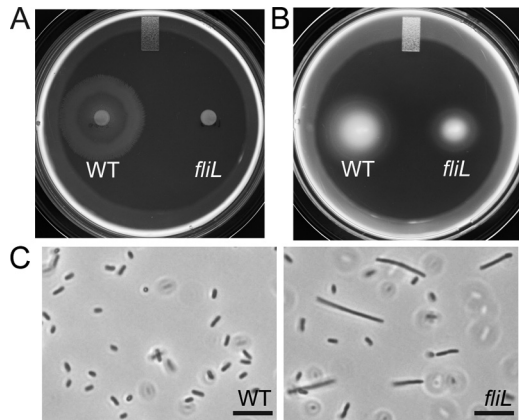


FIG 1 Phenotypic characterization of *fliL* strain YL1003. (A) Swarming motility on LB agar. (B) Swimming motility through semisolid Mot agar. (C) Phase-contrast micrographs of cells obtained from LB broth after 2.75 h of incubation. Scale bar, 10 μm . WT, wild type.

Hamamatsu Orca-R2 CCD camera, and analyzed with Volocity, version 6.1.1, software (PerkinElmer).

Production of pseudoswarmers in 2.75-h broth cultures in a wet-mount sample of living cells was also examined using phase-contrast light microscopy with an Olympus BX60. Phase-contrast images were captured with a QImaging QCam charge-coupled-device (CCD) camera and analyzed with Volocity, version 6.1.1, software.

As previously described (12), a cell length of $>7 \mu\text{m}$ was used as the cutoff to define a swimmer cell. At least five fields (>500 cells) of phase-contrast images and more than 100 fluorescently stained cells of each sample were examined. The mean and standard deviation of the cell length of each cell type were calculated using Prism, version 4.0, software (GraphPad).

RESULTS

Phenotype of *fliL* knockout strains. Swimming and swarming motility were measured in a *fliL* knockout strain (YL1003; *fliL::kan-nt30*). Due to the nature of the mutation, YL1003 has the potential to encode no more than a highly truncated peptide, MS NYSNERKSVK, lacking the TM domain of FliL and making it highly unlikely that the FliL peptide is functional and equally unlikely that it localizes to the inner membrane or periplasm, unlike wild-type FliL.

Analysis of the swarming and swimming motility of YL1003 demonstrated that this *fliL* knockout strain was unable to swarm (Fig. 1A) but was able to swim in semisolid Mot agar (Fig. 1B); i.e., it has an $\text{Swr}^- \text{Swm}^+$ phenotype although the swimming motility is substantially reduced (migration distances are 33.5 mm for the wild type and 21.0 mm for *fliL* cells in Fig. 1B). These results demonstrate that FliL is essential for *P. mirabilis* swarming but not for its swimming. When grown in broth, YL1003 produces pseudoswarmer cells (Elo^+) (Fig. 1C, right panel), with a mean length of $9.49 \pm 2.33 \mu\text{m}$. When grown on nutrient agar, consistent with our previous observation (32), the *fliL* mutant produces elongated cells with a mean cell length equal to or greater than that of the wild-type swimmer cells (data not shown). Maximal production of YL1003 pseudoswarmer cells occurs between 2.5 and 3 h, and these elongated cells comprise a small part (2.1% by number) of the population. Both observations are consistent with previous reports describing *P. mirabilis fliL* mutations (22). It should be remembered that pseudoswarmer cells are longer than wild-type

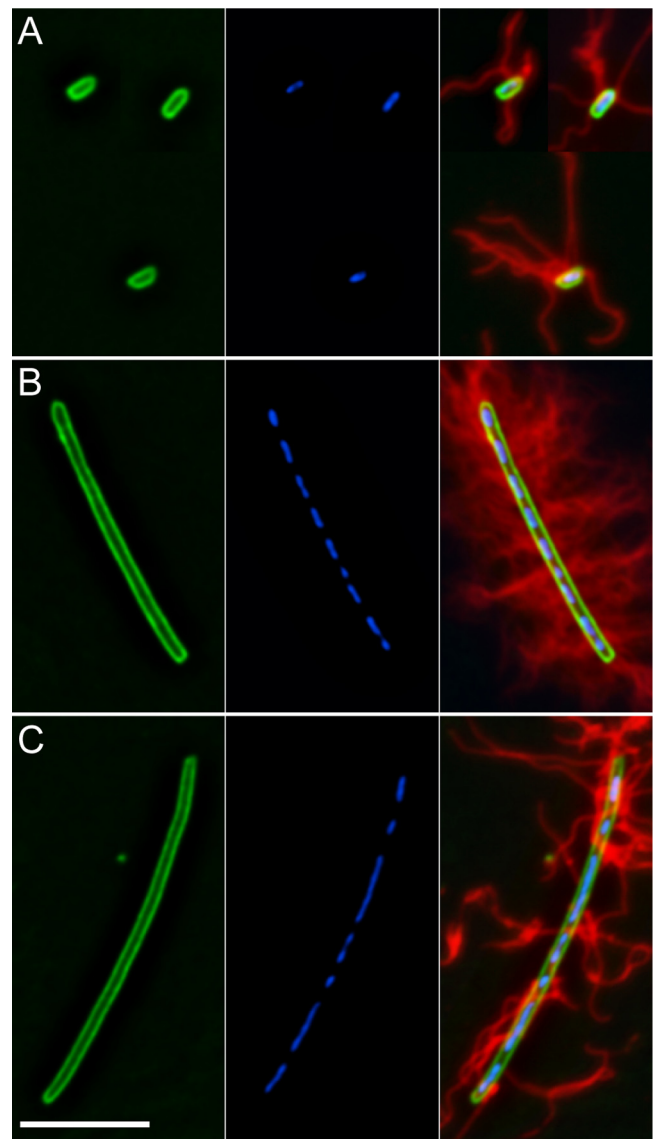


FIG 2 Comparison of *fliL* pseudoswarmer cells to wild-type swimmer and swimmer cells. (A) BB2000 swimmer cells. (B) BB2000 swimmer cell. (C) YL1003 pseudoswarmer cell. From left to right, membrane (FM1-43; green), nucleoids (DAPI; blue), and composite with flagellum immunostaining in red. Scale bar, 7 μm .

swimmer cells; therefore, in terms of swimmer cell equivalents, *fliL* pseudoswarmers represent ca. 10 to 25% of the population of swimmer cells.

While pseudoswarmer cells are similar to wild-type swimmer cells in length, we do not know if they possess other hallmarks of swimmer cells, specifically, multiple nucleoids, lack of septa, and many flagella. To better characterize the pseudoswarmer cells, immunofluorescence microscopy was used to observe the cell membrane, nucleoids, and flagella, comparing these characteristics to wild-type swimmer and swimmer cells. As shown in Fig. 2, wild-type swimmer cells are short rods (average length, $2.26 \pm 0.6 \mu\text{m}$) with a single nucleoid per cell (Fig. 2A) and have distinct septa during division (data not shown). In contrast, wild-type swimmer cells (Fig. 2B) are elongated (average length, $9.79 \pm 3.16 \mu\text{m}$) cells,

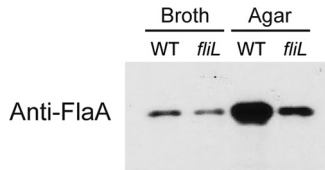


FIG 3 Immunoblot with polyvalent antibodies to flagellin (FlaA). BB2000 (WT) and YL1003 (*fliL*) cells were harvested from LB broth or agar.

possess multiple, evenly spaced nucleoids along the length of the cytoplasm, lack septa, and are covered with many flagella. *fliL* pseudoswarmer cells (Fig. 2C) resemble wild-type swarmer cells in that they are elongated (average length, $9.49 \pm 2.33 \mu\text{m}$), have multiple nucleoids, and lack septa. However, *fliL* pseudoswarmer cells have far fewer flagella than wild-type swarmer cells.

We found it difficult to accurately count the flagella on swarmer and pseudoswarmer cells due to multiple overlapping and clumping filaments. To overcome this problem, the relative amount of flagellin per microgram of total cellular protein was determined using immunoblotting against FlaA (flagellin). Measuring differences in band intensity, we observed that wild-type swarmer cells possess 5.25 times more FlaA than swimmer cells (Fig. 3). In contrast, YL1003 pseudoswarmer cells have the same amount of FlaA per total cell protein as swimmer cells. Growth on nutrient agar increased FlaA levels in YL1003 cells; however, the increase was much less than the 5.25-fold increase seen in wild-type cells. We conclude that *fliL* pseudoswarmer cells are similar but not identical to swarmer cells, with the lack of the hyperflagellated phenotype being the most notable difference.

The expression of representative flagellar genes from each class in the regulatory hierarchy was measured to determine if a reduction in transcription was responsible for the lack of flagella on *fliL* pseudoswarmer cells (Fig. 4). As expected, the *flaA* expression level decreased in *fliL* pseudoswarmer cells compared to the level in the wild type, especially when measured from cells grown on nutrient agar, where a 5-fold decrease in *flaA* levels in pseudoswarmer cells was noted. Much less of a change in *flaA* transcription was observed (0.9-fold less than in wild-type swimmer cells) in broth-grown *fliL* cells. Thus, a decrease in *flaA* transcription helps to explain why pseudoswarmer cells have few flagella.

While *flaA* expression decreased in *fliL* cells, transcription of other flagellar genes, including *flhD*, *fliA*, *fliM*, and *fliO*, increased

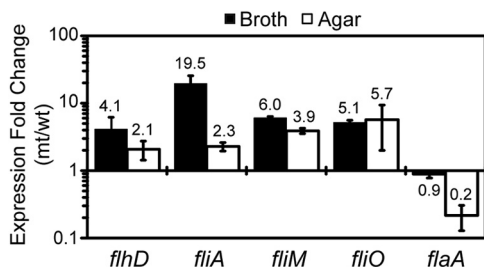


FIG 4 Expression of flagellar genes in *fliL* cells. Values are a comparison of expression of the target gene in *fliL* cells (mt) to the same gene in wild-type (wt) cells. A value of >1 -fold change indicates that expression of the gene is greater in the *fliL* cells than in the wild-type cells, while a value of <1 means that expression decreases in *fliL* cells. Growth media are as indicated on the figure. Means and standard deviations for three independent measurements from three biological samples are shown.

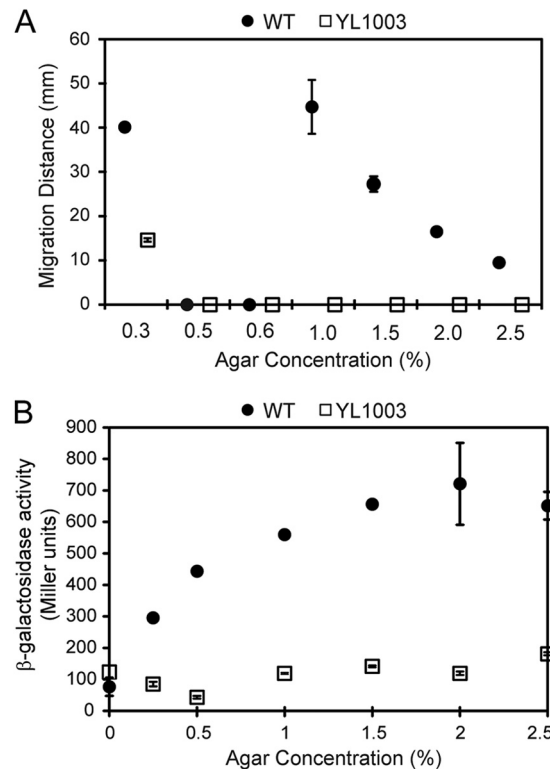


FIG 5 Motility and *flaA* expression in *fliL* cells (YL1003) and wild-type (WT) cells (BB2000) as a function of the viscosity of the medium. (A) Swimming (0.3% agar) or swarming (1.0 to 2.5% agar) as the distance (mm) the cells moved after 5 h. (B) *flaA* (flagellin) expression, measured as β -galactosidase activity from a $P_{flaA}::lacZ$ transcriptional fusion. Means \pm standard deviations are shown.

significantly, compared to wild-type expression (Fig. 4). Although *flaA* transcription decreased, expression of *flhD* and *fliA*, encoding the flagellar master transcriptional activator and sigma factor, respectively, increased in YL1003 compared to wild-type levels (2.1- to 4.1-fold for *flhD*; 2.3- to 19.5-fold for *fliA*). Similar increases in expression of *fliM* and *fliO* (both class II genes) are also evident in pseudoswarmer cells taken from either broth or agar culture (Fig. 4). One interpretation of these results is that *fliL* defects somehow repress or inhibit the positive transcriptional activation of *flaA* by FlhD₄C₂ and FliA while not affecting transcription of other flagellar biosynthetic genes (see Discussion).

FliL functions to enhance motility in viscous environments.

The current model of FliL function suggests that it is required to maintain flagellar structural integrity when torsional stress increases due to external conditions that prevent rotation of the flagella. We tested the hypothesis that *fliL* defects would prevent *P. mirabilis* from responding to the surface signal (in this case, the viscosity of the medium). This was done by measuring swimming and swarming motility of wild-type and YL1003 cells in nutrient broths with different concentrations of agar. The results are shown in Fig. 5A and Table S1 in the supplemental material. As predicted, wild-type cells showed proficient swarming, which was maximal on 1.0% agar (44.7 ± 6.1 mm) and declined as the concentration of agar increased. Wild-type *P. mirabilis* did not swarm at agar concentrations of 0.6% or lower; instead, as the concentration decreased, the cells transitioned to swimming through the

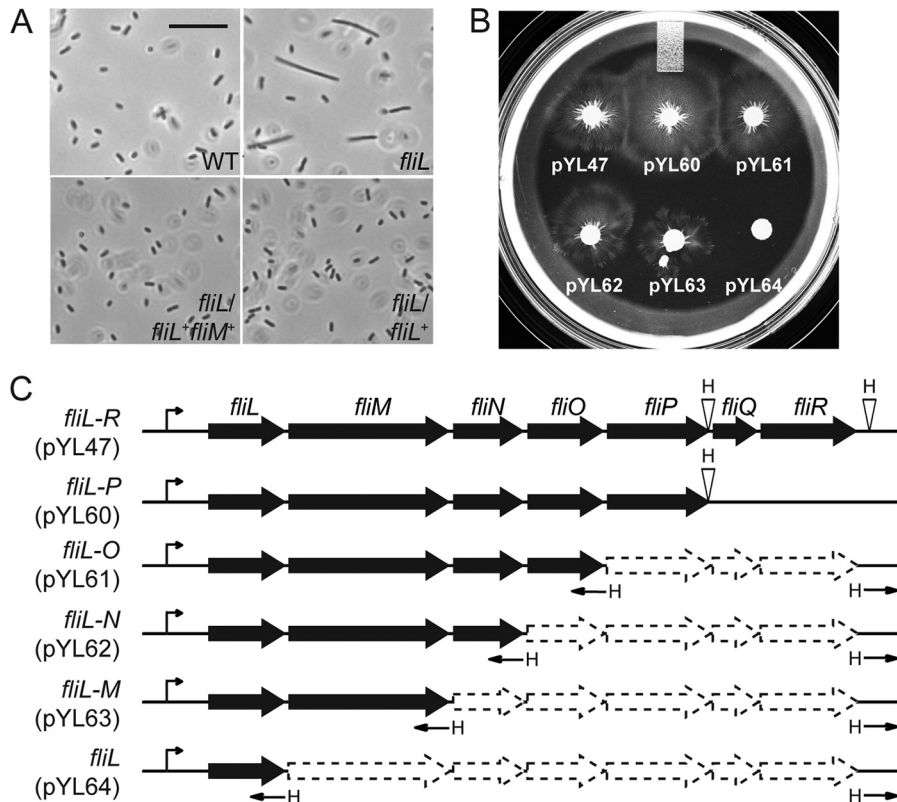


FIG 6 Complementation of *fliL* cells by plasmids bearing deletions of the *fliL* operon. (A) Phase-contrast microscopy to detect pseudoswarmer cells. Scale bar, 20 μm . (B) Swarming motility on LB agar. (C) Sequential deletion of the *fliL* operon resulted in six plasmids, each harboring one less gene starting from the 3' end of the operon. This yielded pYL47 (*fliL* to *fliR*), pYL60 (*fliL* to *fliP*), pYL61 (*fliL* to *fliO*), pYL62 (*fliL* to *fliN*), pYL63 (*fliL* to *fliM*), and pYL64 (*fliL*). All plasmids contain the native *fliL* promoter (P_{fliL}; arrows in front of *fliL*). HindIII sites are indicated by H.

agar matrix. In contrast, YL1003 cells did not swarm at any agar concentration and were less able to swim through 0.3% agar (Fig. 5A; see also Table S1). These results show that *P. mirabilis* swarms in a viscosity-dependent manner and demonstrate a link between viscosity and FliL function.

In parallel experiments, *flaA* expression was measured in wild-type and YL1003 cells over the same concentrations of agar. While expression of *flaA* rose in wild-type cells as the concentration of agar in the medium increased, *fliL* cells showed no change in *flaA* transcription (Fig. 5B). Thus, loss of FliL function prevents increased *flaA* expression that would normally result from the surface-sensing events.

Complementation of the *fliL* knockout requires the *fliL* coding sequence, the *fliL* promoter region, and sequences in the *fliM* coding region. The *fliL* phenotype has two characteristics: inability to swarm (Swr⁻ phenotype) and pseudoswarmer formation (Elo⁺). We attempted to complement the *fliL* phenotype of YL1003 by introducing plasmids carrying the *fliL* coding region transcribed from either the *fliL* promoter (P_{fliL}::*fliL*⁺), an IPTG-inducible promoter (P_{trc}::*fliL*⁺), or an arabinose-inducible promoter (P_{BAD}::*fliL*⁺). With all three plasmids, the Elo⁺ phenotype was complemented, returning YL1003 to swimmer cell morphology (Fig. 6A, compare the upper right with the bottom right panel). However, none of these plasmids was able to complement the Swr⁻ phenotype, and the cells remained nonswarming. Our results show that the elongation and swarming phenotypes in the *fliL* mutant are separable, based on the complementation data. *fliL*

transcripts were detectable from all three promoters (data not shown). Thus, the failure to complement the complete *fliL* phenotype of YL1003 is not due to a failure of *fliL* transcription in *trans*.

Motelab et al. suggested that *Borrelia* FliL functionality is sensitive to *fliL* copy number (26), which led us to test whether complementation of YL1003 could be achieved by expressing P_{fliL}::*fliL* from an ectopic chromosomal site. In an unrelated study, we discovered that a knockout of PMI3101 (encoding the sole GGDEF protein in *P. mirabilis*) did not affect any measurable phenotype (data not shown), making this gene an excellent site for integration of P_{fliL}::*fliL*. A single-crossover, Campbell-style integration was performed, and the exconjugants were screened for swarming (see Materials and Methods). Six Swr⁺ exconjugants were found, but none had P_{fliL}::*fliL* integrated at PMI3101. Instead, in all six exconjugants, single-crossover recombination events occurred at the native *fliL* codon region, leading to a resurrection of a wild-type *fliLMNOPQR* operon and resulting in Swr⁺ bacteria. This was unexpected since statistical probability would be predicted to favor a crossover at the PMI3101 locus due to the much larger target (1.5 kb) it represents than the *fliL* target (<500 bp).

Although we do not fully understand why the recombination at *fliL* occurred, we inferred from this result that complementation of the Swr⁻ phenotype in YL1003 required DNA beyond the *fliL* promoter and coding region. To test this hypothesis, a DNA fragment containing the *fliL* operon (*fliLMNOPQR*) transcribed from its native *fliL* promoter (P_{fliL}) was placed on a plasmid, and the

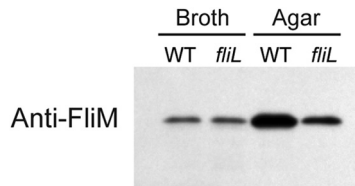


FIG 7 Immunoblotting with polyvalent antibodies to FliM. BB2000 (WT) and YL1003 (*fliL*) cells were harvested from LB broth or agar. The antiserum used was directed against *E. coli* FliM and cross-reacts with *P. mirabilis* FliM.

resulting plasmid pYL47 was moved into YL1003. In agreement with the hypothesis, pYL47 containing the *fliL* operon restored swarming of YL1003 (Fig. 6B).

Complementation of the Swr^- phenotype in YL1003 is not due to loss of transcription of genes downstream from *fliL*. This was demonstrated in the results shown in Fig. 4 (expression of *fliM* and *fliO*). The abundance of FliM was also measured to verify that YL1003 was able to translate the proteins of the *fliL* operon, without FliL (Fig. 7). Indeed, the amount of FliM in YL1003 is identical to that of wild-type cells when they are grown in broth and decreased slightly when *fliL* cells are grown on agar medium (Fig. 7). These results suggested to us that complementation of the Swr^- phenotype of YL1003 required *fliL* operon DNA beyond the *fliL* promoter and coding region.

A set of plasmids bearing deletions in the *fliL* operon was made (Fig. 6C) and used to complement YL1003. Plasmids bearing *fliL* and *fliM* (pYL60, pYL61, pYL62, and pYL63 in Fig. 6B) returned YL1003 to an Swr^+ phenotype, but loss of *fliM* DNA (pYL64) could not restore swarming to the *fliL* cells. As shown in Fig. 6B, the swarming diameters of YL1003 containing pYL47, pYL60, pYL61, pYL62, and pYL63 are, respectively, 20.7 mm, 29.7 mm, 22.5 mm, 20.7 mm, and 18.9 mm. As expected, both pYL63 (*fliL*⁺ *fliM*⁺) and pYL64 (*fliL*⁺) complemented the Elo^+ phenotype of YL1003 (Fig. 6A). Therefore, complementation of *fliL* requires three things: the *fliL* promoter region, the *fliL* coding region, and DNA within the *fliM* coding region.

Expressing *fliLM* in trans improves *fliL* motility. The complementation results predict that $P_{fliL}::fliLM$ cells would regain viscosity-dependent swarming. We measured swarming over various agar concentrations (as previously performed) and found that *fliL*⁺ *fliM*⁺, but not *fliL*⁺ alone, restored swarming of YL1003 on 1.0 and 1.5% agar surfaces in a viscosity-dependent manner (see Table S1 in the supplemental material). YL1003 (*fliL*⁺ *fliM*⁺) is not proficient in swarming (i.e., longer lag and lower rate than wild-type cells), but its overall response to viscosity is the same (see Table S1). Both have maximal swarming in 1.0% agar, the maximal swarming rates for each are as fast as the swimming rate (in 0.3% agar), and their swarming rates both decrease in the same degree (0.4- to 0.5-fold) when the agar concentration increases from 1.0% to 1.5%. Prolonged incubation of the complemented YL1003 cells did not restore swarming.

The *fliL*⁺ *fliM*⁺ complementation results predict that YL1003/pYL63 (*fliL*⁺ *fliM*⁺) has regained wild-type flagellin synthesis, and this was measured by Western blotting of cells obtained after growth on nutrient agar (Fig. 8). As predicted, complementation with *fliL*⁺ *fliM*⁺ increased the overall production of flagellin, compared to *fliL* cells or YL1003/pYL64 (*fliL*⁺). There is a noticeable difference in attached (pellet fraction) and unattached (su-

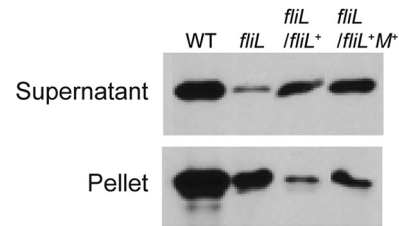


FIG 8 Immunoblot measuring the abundance of detached and attached flagella in *fliL* cells complemented with *fliL*⁺ or *fliL*⁺ *fliM*⁺. Wild-type and *fliL* cells were harvested after 4.5 h of incubation on LB agar. Rabbit polyvalent antiserum to FlaA was used, as described in the legend of Fig. 3.

pernatant) flagella in these cells. In addition to increasing the overall abundance of FlaA, complementation of YL1003 with *fliL*⁺ *fliM*⁺ also increases the number of attached flagella per cell (compare *fliL*/*fliL*⁺ *fliM*⁺ with *fliL*/*fliL*⁺), which is reasonable since FliL is required to maintain the integrity of the flagellar rod. The surprise is that FliL function also requires *fliM* DNA.

DISCUSSION

Most, if not all, bacteria are able to live either as independent planktonic cells or as members of organized surface-anchored communities called biofilms (46). Biofilm formation is a developmental process that begins when a motile bacterium attaches to a surface and requires bacterial processes. One such process is flagellum-mediated motility, which facilitates attachment to and colonization of surfaces. However, while it is generally agreed that motility and biofilm development are mutually exclusive, the molecular mechanisms that underlie the swim-or-stick lifestyle switch remain virtually unknown for most bacterial species.

The long-term goal of our laboratory is to understand the molecular mechanism involved in how *P. mirabilis* senses a surface. The results from the current study further implicate FliL as a major player in the swim-or-stick mechanism of the swarming bacterium *P. mirabilis*. Our previous studies used a pseudoswarmer-producing strain containing a transposon insertion (*fliL*::Tn5) at nucleotide 440 in *fliL* (32). This strain has an $\text{Swm}^- \text{Swr}^-$ phenotype due to polar effects of the transposon on downstream genes in the *fliL* operon, which in turn decreases expression of flagellar class III genes, e.g., *flaA*, and prevents flagellar biosynthesis (12). Furthermore, due to the transposon, this strain has a frameshift in the 3' end of *fliL* such that the mutant retains most (>90%) of the wild-type *fliL* sequence. Both the polar effects on the *fliL* operon and the frameshift of *fliL* are disadvantageous for studying FliL function. To overcome these drawbacks, in the present study, we constructed a nonpolar *fliL* null mutation by site-specific Targetron insertion at nucleotide 30, a site chosen to result in a highly truncated FliL, thereby eliminating the problems associated with the use of the *fliL*::Tn5 strain. As we along with others have shown, defects in *fliL* abolish swarming and reduce swimming motility. Decreased swimming of *fliL*::*kan*-nt30 cells is due to decreased flagella/flagellin production (compared to wild-type cells) when cells are grown in semisolid nutrient agar (Fig. 5B). This does not suggest that broth-grown FliL⁻ cells lack a phenotype because their morphology is highly similar to a wild-type swarmer cell. These pseudoswarmer cells, as we call them, are elongated, non-septated rods, with multiple nucleoids (Fig. 2). Using only these criteria, there is no difference between a wild-type swarmer cell

and a *fliL* pseudoswarmer from broth culture. This leads us to conclude that loss of FliL inappropriately flips the swim-or-stick switch such that the bacterium responds as though it is on a surface, despite being in a noninducing environment, i.e., nutrient broth. However, it is not as simple as that.

Unlike swarmer cells, pseudoswarmer cells are not hyperflagellated, with roughly the same number of flagella per μm^2 as wild-type swimmer cells (Fig. 2 and 3), indicating a major difference between *fliL* pseudoswarmer cells and wild-type swarmer cells. This difference occurs at the level of *flaA* expression that translates to a smaller amount of FlaA per cell. Oddly, while *flaA* (a flagellar class III gene) transcription decreases in pseudoswarmer cells, expression of *flhD* (class I) and *fliA* (class II) increases. Although the mechanism is not immediately apparent, an increase in *flhD* expression makes sense as it parallels upregulation of *flhD* transcription observed when swimmer cells differentiate into swarmer cells (21). The disparity in *flhD* and *fliM* expression levels on agar between the *fliL::kan-nt30* and *fliL::Tn5* mutants is certainly due to the aforementioned polar effect and *fliL* frameshift.

Why does *fliA* expression increase? Since FliA, the flagellar gene sigma factor, is required for *flaA* expression (47), an increase in FliA should result in an increase in FlaA, yet the opposite occurs. An increase in FlhD₄C₂ is expected to increase *fliA* expression, offering a partial explanation for these results. While a complete explanation for this reproducible event is not immediately evident, it is obvious that loss of FliL, a structural gene, results in an increase in the transcription of two flagellar regulatory genes. This could occur if loss of FliL somehow damaged the flagellar type III secretion system, which would prevent export of FlgM, the flagellar anti-sigma factor, inhibit the activity of FliA, and result in a decrease in class III gene expression. This hypothesis predicts that the expression of other class III flagellar genes is also low in pseudoswarmers, and experiments are under way to determine if this is true.

P. mirabilis senses a surface by monitoring the rotation of its swimmer cell flagella (32). As flagellum movement becomes inhibited by conditions that prevent rotation, e.g., viscosity of the medium, a signal is sent that activates transcription of a set of genes that produce swarmer cells (3, 12, 13, 32, 48, 49). Based on this knowledge, we predicted that *fliL* cells would be blind to changes in the viscosity of the medium and would be unable to sense (or respond to) the stimulus and unable to swarm (even on low concentrations of agar). Indeed, this is exactly what was seen. YL1003 did not swarm on any agar medium, while wild-type cells swarmed on concentrations of agar up to 2.5%, the highest we tested (Fig. 5A). Furthermore, both wild-type and *fliL* cells swam through semisolid agar matrices, albeit *fliL* cells migrated through the agar at less than half the rate of wild-type cells. As predicted, expression of *flaA* increased in wild-type cells roughly in step with increased agar concentration (Fig. 5B) and reached a plateau around 2.0% agar, while transcription of *flaA* in YL1003 remained at a basal level throughout the agar concentration series. The pseudoswarmer phenotype, but not the swarming defect, of *fliL* cells is rescued by *fliL* alone (Fig. 6A); therefore, *fliL* cells reveal that cell elongation and the swarming phenotypes are separable characteristics. The *fliL* mutant constitutively produced elongated pseudoswarmer cells under noninducing conditions, demonstrating that the loss of FliL affects not only swarming, due to the defect in *flaA* expression, but also the ability of the cell to detect surfaces, as the mutant “thinks” it is on a surface when it is not. Thus, defects in

fliL affect the ability of the cells to sense surfaces. We believe that this hints at two functions for FliL: maintenance of flagellum integrity and involvement in surface signaling.

Figure 5A also reveals another interesting result: wild-type *P. mirabilis* is incapable of either swimming or swarming at agar concentrations between 0.5 and 0.6%. One reasonable interpretation is that these concentrations of agar are too high for swimming and too low to induce swarmer cell differentiation, presumably because they do not produce adequate torsional forces on the flagellar motor. This is supported by observations that swarmer cells are not observed on either 0.5 or 0.6% agar (data not shown).

Breakage of flagella occurs in both wild-type and *fliL* cells (Fig. 8), emphasizing that movement over agar increases the probability of flagellar damage. We also observed that when *fliL* cells are complemented by *fliL*⁺ *fliM*⁺ but not by *fliL*⁺ alone, the ratio of attached to unattached flagella decreased, and more flagella were attached to the *fliL*⁺ *fliM*⁺ cells. While this observation underscores the requirement of FliL in maintaining flagellar integrity, it also highlights one of the most interesting of our results that an extragenic nucleotide sequence within the *fliM* coding region is required for maximal FliL activity (Fig. 6 and 8).

It comes as a surprise that complementation of the Swr⁻ phenotype in *fliL* cells requires the *fliL* promoter (including the 5' untranslated region [UTR]), *fliL* coding region, and a portion of *fliM* DNA (Fig. 6). The results rule out the possibility that requirement of *fliM* is due to defects in *fliM* expression (transcription or translation) in YL1003 (Fig. 4 and 7). We also have preliminary evidence that full FliL function requires <200 bp of the 5' end of *fliM* (unpublished data). It is tempting to speculate that a *cis*-acting factor located in *fliM* is acting to enhance or control FliL function, perhaps working in a similar manner to the antisense RNA that overlaps the *fliL* operon of *Salmonella* (50). Studies are in progress to determine the molecular mechanism behind the *fliM* DNA requirement.

ACKNOWLEDGMENTS

We thank David Blair for the gift of FliM antibody, Brian Youchak for assisting with the swarming assay, Rayford Payne for comments on the manuscript, and members of Belas Laboratory for helpful discussion.

J.P. is supported by the Meyerhoff Scholars Program at University of Maryland Baltimore County. This work was supported by award MCB-0919820 from the National Science Foundation.

REFERENCES

- Mobley HL, Belas R. 1995. Swarming and pathogenicity of *Proteus mirabilis* in the urinary tract. *Trends Microbiol.* 3:280–284.
- Rozalski A, Sidorczyk Z, Kotelko K. 1997. Potential virulence factors of *Proteus bacilli*. *Microbiol. Mol. Biol. Rev.* 61:65–89.
- Alavi M, Belas R. 2001. Surface sensing, swarmer cell differentiation, and biofilm development. *Methods Enzymol.* 336:29–40.
- Belas R, Erskine D, Flaherty D. 1991. *Proteus mirabilis* mutants defective in swarmer cell differentiation and multicellular behavior. *J. Bacteriol.* 173:6279–6288.
- Allison C, Lai HC, Hughes C. 1992. Co-ordinate expression of virulence genes during swarm-cell differentiation and population migration of *Proteus mirabilis*. *Mol. Microbiol.* 6:1583–1591.
- Henrichsen J. 1972. Bacterial surface translocation: a survey and a classification. *Bacteriol. Rev.* 36:478–503.
- Hoeniger JF. 1966. Cellular changes accompanying the swarming of *Proteus mirabilis*. II. Observations of stained organisms. *Can. J. Microbiol.* 12:113–123.
- Kearns DB. 2010. A field guide to bacterial swarming motility. *Nat. Rev. Microbiol.* 8:634–644.
- Allison C, Coleman N, Jones PL, Hughes C. 1992. Ability of *Proteus*

- mirabilis* to invade human urothelial cells is coupled to motility and swarming differentiation. *Infect. Immun.* 60:4740–4746.
10. Coker C, Poore CA, Li X, Mobley HL. 2000. Pathogenesis of *Proteus mirabilis* urinary tract infection. *Microbes Infect.* 2:1497–1505.
 11. Jacobsen SM, Stickler DJ, Mobley HL, Shirliff ME. 2008. Complicated catheter-associated urinary tract infections due to *Escherichia coli* and *Proteus mirabilis*. *Clin. Microbiol. Rev.* 21:26–59.
 12. Cusick K, Lee YY, Youchak B, Belas R. 2012. Perturbation of FliI interferes with *Proteus mirabilis* swarmer cell gene expression and differentiation. *J. Bacteriol.* 194:437–447.
 13. Pearson MM, Rasko DA, Smith SN, Mobley HL. 2010. Transcriptome of swarming *Proteus mirabilis*. *Infect. Immun.* 78:2834–2845.
 14. Apel D, Surette MG. 2008. Bringing order to a complex molecular machine: the assembly of the bacterial flagella. *Biochim. Biophys. Acta* 1778:1851–1858.
 15. Chevance FF, Hughes KT. 2008. Coordinating assembly of a bacterial macromolecular machine. *Nat. Rev. Microbiol.* 6:455–465.
 16. Komeda Y. 1982. Fusions of flagellar operons to lactose genes on a μ *lac* bacteriophage. *J. Bacteriol.* 150:16–26.
 17. Kutsukake K, Ohya Y, Iino T. 1990. Transcriptional analysis of the flagellar regulon of *Salmonella typhimurium*. *J. Bacteriol.* 172:741–747.
 18. Macnab RM. 1996. Flagella and motility, p 123–145. In Neidhardt FC, Ingraham JL, Low KB, Magasanik B, Schaechter M, Umberger HE (ed), *Escherichia coli* and *Salmonella*: cellular and molecular biology. American Society for Microbiology Press, Washington, DC.
 19. Liu X, Matsumura P. 1996. Differential regulation of multiple overlapping promoters in flagellar class II operons in *Escherichia coli*. *Mol. Microbiol.* 21:613–620.
 20. Liu X, Matsumura P. 1994. The FlhD/FlhC complex, a transcriptional activator of the *Escherichia coli* flagellar class II operons. *J. Bacteriol.* 176:7345–7351.
 21. Furness RB, Fraser GM, Hay NA, Hughes C. 1997. Negative feedback from a *Proteus* class II flagellum export defect to the *flhDC* master operon controlling cell division and flagellum assembly. *J. Bacteriol.* 179:5585–5588.
 22. Pruss BM, Matsumura P. 1996. A regulator of the flagellar regulon of *Escherichia coli*, *flhD*, also affects cell division. *J. Bacteriol.* 178:668–674.
 23. Kihara M, Homma M, Kutsukake K, Macnab RM. 1989. Flagellar switch of *Salmonella typhimurium*: gene sequences and deduced protein sequences. *J. Bacteriol.* 171:3247–3257.
 24. Attmannspacher U, Scharf BE, Harshey RM. 2008. FliI is essential for swarming: motor rotation in absence of FliL fractures the flagellar rod in swarmer cells of *Salmonella enterica*. *Mol. Microbiol.* 68:328–341.
 25. Schoenhals GJ, Macnab RM. 1999. FliL is a membrane-associated component of the flagellar basal body of *Salmonella*. *Microbiology* 145:1769–1775.
 26. Motaleb MA, Pitzer JE, Sultan SZ, Liu J. 2011. A novel gene inactivation system reveals altered periplasmic flagellar orientation in a *Borrelia burgdorferi* *fliL* mutant. *J. Bacteriol.* 193:3324–3331.
 27. Belas R, Horikawa E, Aizawa S, Sivanasuthi R. 2009. Genetic determinants of *Silicibacter* sp. TM1040 motility. *J. Bacteriol.* 191:4502–4512.
 28. Jenal U, White J, Shapiro L. 1994. *Caulobacter* flagellar function, but not assembly, requires FliL, a non-polarly localized membrane protein present in all cell types. *J. Mol. Biol.* 243:227–244.
 29. Suaste-Olmos F, Domenzain C, Mireles-Rodriguez JC, Poggio S, Osorio A, Dreyfus G, Camarena L. 2010. The flagellar protein FliI is essential for swimming in *Rhodobacter sphaeroides*. *J. Bacteriol.* 192:6230–6239.
 30. Raha M, Sockett H, Macnab RM. 1994. Characterization of the *fliL* gene in the flagellar regulon of *Escherichia coli* and *Salmonella typhimurium*. *J. Bacteriol.* 176:2308–2311.
 31. Berg HC, Turner L. 1993. Torque generated by the flagellar motor of *Escherichia coli*. *Biophys. J.* 65:2201–2216.
 32. Belas R, Sivanasuthi R. 2005. The ability of *Proteus mirabilis* to sense surfaces and regulate virulence gene expression involves FliL, a flagellar basal body protein. *J. Bacteriol.* 187:6789–6803.
 33. Belas R, Erskine D, Flaherty D. 1991. Transposon mutagenesis in *Proteus mirabilis*. *J. Bacteriol.* 173:6289–6293.
 34. Davanloo P, Rosenberg AH, Dunn JJ, Studier FW. 1984. Cloning and expression of the gene for bacteriophage T7 RNA polymerase. *Proc. Natl. Acad. Sci. U. S. A.* 81:2035–2039.
 35. Amann E, Ochs B, Abel KJ. 1988. Tightly regulated *tac* promoter vectors useful for the expression of unfused and fused proteins in *Escherichia coli*. *Gene* 69:301–315.
 36. Guzman LM, Belin D, Carson MJ, Beckwith J. 1995. Tight regulation, modulation, and high-level expression by vectors containing the arabinose P_{BAD} promoter. *J. Bacteriol.* 177:4121–4130.
 37. Chang AC, Cohen SN. 1978. Construction and characterization of amplifiable multicopy DNA cloning vehicles derived from the P15A cryptic miniplasmid. *J. Bacteriol.* 134:1141–1156.
 38. Miller VL, Mekalanos JJ. 1988. A novel suicide vector and its use in construction of insertion mutations: osmoregulation of outer membrane proteins and virulence determinants in *Vibrio cholerae* requires *toxR*. *J. Bacteriol.* 170:2575–2583.
 39. Sambrook J, Russell DW. 2001. *Molecular cloning: a laboratory manual*, 3rd ed. Cold Spring Harbor Laboratory Press, Cold Spring Harbor, NY.
 40. Zhong J, Karberg M, Lambowitz AM. 2003. Targeted and random bacterial gene disruption using a group II intron (Targetron) vector containing a retrotransposition-activated selectable marker. *Nucleic Acids Res.* 31:1656–1664.
 41. Heery DM, Powell R, Gannon F, Dunican LK. 1989. Curing of a plasmid from *E. coli* using high-voltage electroporation. *Nucleic Acids Res.* 17:10131.
 42. Livak KJ, Schmittgen TD. 2001. Analysis of relative gene expression data using real-time quantitative PCR and the $2^{-\Delta\Delta CT}$ method. *Methods* 25:402–408.
 43. Simons RW, Houtman F, Kleckner N. 1987. Improved single and multicopy *lac*-based cloning vectors for protein and operon fusions. *Gene* 53:85–96.
 44. Miller JH. 1992. *A short course in bacterial genetics*. Cold Spring Harbor Laboratory Press, Cold Spring Harbor, NY.
 45. Lee YY, Barker CS, Matsumura P, Belas R. 2011. Refining the binding of the *Escherichia coli* flagellar master regulator, FlhD₄C₂, on a base-specific level. *J. Bacteriol.* 193:4057–4068.
 46. Hall-Stoodley L, Stoodley P. 2005. Biofilm formation and dispersal and the transmission of human pathogens. *Trends Microbiol.* 13:7–10.
 47. Belas R, Flaherty D. 1994. Sequence and genetic analysis of multiple flagellin-encoding genes from *Proteus mirabilis*. *Gene* 148:33–41.
 48. Rather PN. 2005. Swarmer cell differentiation in *Proteus mirabilis*. *Environ. Microbiol.* 7:1065–1073.
 49. Morgenstein RM, Szostek B, Rather PN. 2010. Regulation of gene expression during swarmer cell differentiation in *Proteus mirabilis*. *FEMS Microbiol. Rev.* 34:753–763.
 50. Wang Q, Harshey RM. 2009. Rcs signalling-activated transcription of *rcsA* induces strong anti-sense transcription of upstream *fliPQR* flagellar genes from a weak intergenic promoter: regulatory roles for the anti-sense transcript in virulence and motility. *Mol. Microbiol.* 74:71–84.